JACS
JOURNAL OF THE AMERICAN CHEMICAL SOCIETY

Article

pubs.acs.org/JACS

Degenerate Nucleophilic Substitution in Phosphonium Salts

Elizabeth V. Jennings, Kirill Nikitin, Yannick Ortin, and Declan G. Gilheany*

Centre for Synthesis and Chemical Biology, School of Chemistry and Chemical Biology, University College Dublin, Dublin 4, Ireland

Supporting Information

ABSTRACT: Rates and energy barriers of degenerate halide substitution on tetracoordinate halophosphonium cations have been measured by NMR techniques (VT and EXSY) using a novel experimental design whereby a chiral substituent (^{s}Bu) lifts the degeneracy of the resultant salts. Concomitantly, a viable computational approach to the system was developed to gain mechanistic insights into the structure and relative stabilities of the species involved. Both approaches strongly suggest a two-step mechanism of formation of a pentacoordinate dihalophosphorane via backside attack followed by dissociation, resulting in inversion of configuration at phosphorus. The experimentally determined barriers range from <9 kcal mol^{-1} to nearly 20 kcal mol^{-1}, ruling out a mechansm via Berry pseudorotation involving equatorial halides. In all cases studied, epimerization of chlorophosphonium chlorides has a lower energy barrier (by 2 kcal mol^{-1}) than the analogous bromo salts. Calculations determined that this was due to the easier accessibility in solution of pentacoordinate dichlorophosphoranes when compared to analogous dibromophosphoranes. In line with the proposed associative mechanism, bulky substituents slow the reaction in the order Me < Et < ^{i}Pr < ^{t}Bu. Bulky substituents affect the shape of the reaction energy profile so that the pentacoordinate intermediate is destabilized eventually becoming a transition state. The magnitude of the steric effects is comparable to that of the same substituents on substitution at primary alkyl halides, which can be rationalized by the relatively longer P−C bonds. The reaction displays first-order kinetics due to the prevalence of tight- or solvent-separated ion pairs in solution. Three-dimensional reaction potential energy profiles (More O'Ferrall−Jencks plots) indicated a relatively shallow potential well corresponding to the trigonal bipyramid intermediate flanked by two transition states

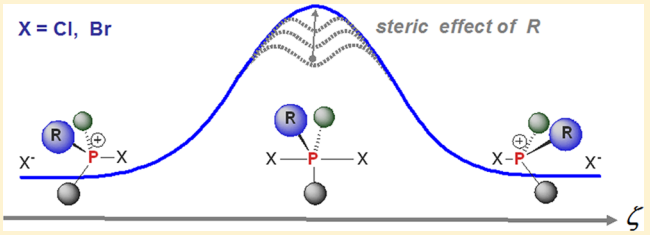

INTRODUCTION

The kinetics and stereochemistry of bimolecular nucleophilic substitution at carbon[1] are well understood[2,3] and have contributed to its widespread use in organic synthesis.[4] Most significantly, whereas dissociative mechanisms typically lead to racemization at a carbon center, associative mechanisms tend to either invert or retain the stereochemistry of the substrate, which has made them powerful tools in asymmetric synthesis. More recent investigations of nucleophilic substitution at carbon, mostly computational, have included its chemical dynamics,[5] the nature of steric effects in substitution reactions, the role of Pauli repulsion therein[6] and the development of more detailed understanding of solvent effects.[7] In all of these contexts, degenerate and pseudodegenerate processes where the nucleophile and leaving group are the same or similar are particularly interesting because they allow monitoring/analysis of the associative mechanism free from effects due to the leaving group.[8]

We are interested in degenerative nucleophilic substitution at phosphonium centers because it became apparent (vide infra) that it played a role in the stereoselectivity of our asymmetric Appel process.[9] The study of nucleophilic substitution at centers other than carbon has been a more recent activity.[10] The trends at silicon are fairly well established and provide an indication of pertinent issues for third-row elements.[11,12] Notably, the stereochemical outcome is determined by the properties of the relatively stable pentacoordinate anionic intermediate formed in an associative mechanism. Inversion will occur if the nucleophile approaches from the opposite side to the leaving group. However, such pentacoordinate intermediates may change their configuration via Berry pseudorotation,[13] and in solution, the pentacoordinate intermediate half-life depends on leaving group ability. Thus, good leaving groups prevent racemization,[14] contrasting with carbon chemistry, where they induce it.

In recent years, the Bickelhaupt group has reported extensively on nucleophilic substitution at phosphorus, both phosphinyl P(III) and phosphoryl O=P(V) centers, and many of their theory/calculation-based discussions also involve comparison to the analogous reactions at carbon and silicon.[7,15,16] The results of their phosphoryl calculations give us some expectations for the behavior of phosphonium systems, especially with regard to the crucial influence of the solvent. In the absence of solvent, which switches the relative stabilities of the pentacoordinate and tetracoordinate states (see Figure 1a), they also found that that substituent effects were notable and can lead to the appearance of a double-maximum PES with two unsymmetrical TSs connected by a short-lived pentacoordinate intermediate (dashed line in Figure 1a).

Received: July 28, 2014
Published: November 11, 2014

   dx.doi.org/10.1021/ja507433g | J. Am. Chem. Soc. 2014, 136, 16217−16226

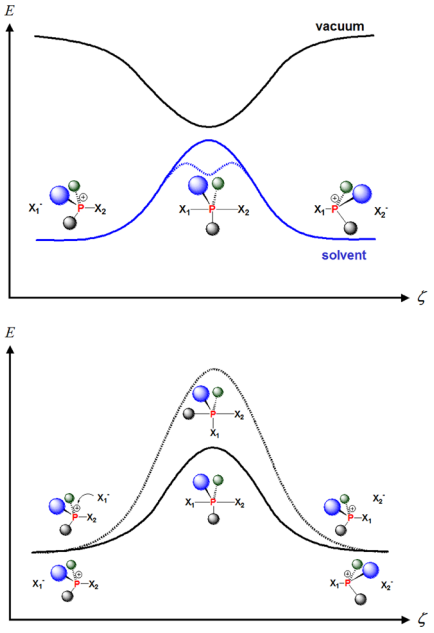

Figure 1. Expected energy profiles of nucleophilic substitution reactions at phosphonium: (a) dramatic change of PES profile in solution can be accompanied by the appearance of a single- or double-maximum (dashed line) barrier; (b) lower energy barrier (solid line) is expected for a reaction via more stable pentacoordinate species in which both electronegative groups **X** occupy axial positions.

Another important factor relevant to the height of the barrier to nucleophilic attack at tetracoordinate phosphorus cation is the apicophilicity of substituents, i.e., their tendency to adopt an axial position in any derived pentacoordinate phosphorus-(V) species.[17] The classic scale of apicophilicity based on experimental data was compiled by Trippet and co-workers[18] and is positively correlated with the electronegativity of atoms or groups. Therefore, displacement of electronegative groups is likely to occur via a diaxial pentacoordinate intermediate (Figure 1b) with inversion of configuration at the phosphorus. It is found that strongly apicophilic nucleophiles tend to invert stereochemistry at phosphorus, whereas weakly apicophilic nucleophiles allow racemization, again due to competition from Berry pseudorotation.[18−20]

Our interest in the phosphonium series arose when we identified certain chiral chlorophosphonium salts (CPS) as crucial intermediates in our dynamic resolution of phosphines and their oxides.[9d,e] Our experimental observations suggested that the CPS undergo fast racemization at the phosphorus center, which in turn is strongly affected by the steric size of adjacent organic groups. Thus, a cornerstone of our hypothesis is a degenerate chlorine-exchange reaction at phosphonium (Figure 2a). Therefore, we sought an experimental approach that would assist our own work, aware that this might also shed a new light on the steric size/reactivity relationship problem. Halophosphonium salts are known reactive intermediates in a number of reactions in phosphorus chemistry and in synthetic organic chemistry.[21] Recent work by ourselves[22] and Denton and co-workers[23] has used such salts as key intermediates in a number of phosphorus functional group interconversions and as reagents in organic synthesis, and we have shown that they can be generated in a number of ways.[24] Dihalides R_3PX_2 (CPS, X = Cl; BPS, X = Br) are known to exist in their tetrahedral ionic form in polar solvents such as DCM and in a

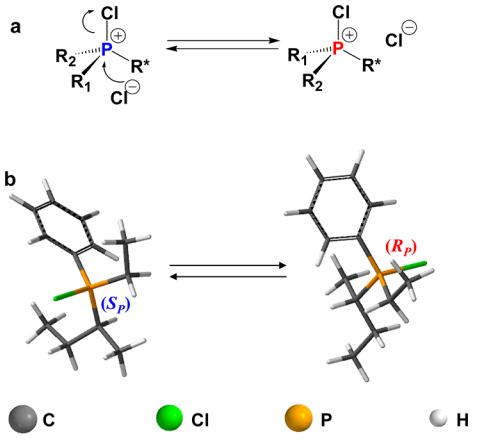

Figure 2. Pseudodegenerate exchange reactions in chlorophosphonium chlorides: (a) enantiomeric *P*-chlorophosphonium cations (R* = achiral group); (b) dynamic interconversion of diastereomeric chlorophosphonim (R* = racemic *s*-Bu).

pentacoordinate neutral form in nonpolar solvents such as benzene.[25] These have widely divergent ^{31}P shifts, negative for the pentacoordinate form, positive for the ionic, tetrahedral form, but otherwise, there are relatively few experimental studies of their general trends in reactivity and dynamic behavior.

Any pentacoordinate intermediate in the substitution of a CPS would have apical chlorines in its most stable configuration, and pseudorotation involving highly disfavored equatorial chlorines—even transiently—should have a high energy barrier (see Figure 1b). Our own measurements (vide infra) and the recent computational work of Bickelhaupt and co-workers for the phosphoryl case suggest that the barrier to the key Walden-type inversion step at phosphorus is low or of medium height (5−25 kcal/mol).[15,16] Therefore, it is reasonable to assume that this reaction proceeds via a pentacoordinate transition state or short-lived intermediate making the process similar and directly comparable to the analogous S_N2 processes in carbon chemistry.[26] The relatively low barrier to inversion also means crucially that the system is susceptible to study by dynamic NMR techniques.

We present here our findings indicating that indeed nucleophilic displacement at the halophosphonium cation occurs with inversion via an ion-pair mediated associative mechanism, complementary to classical carbon chemistry. But, in contrast to carbon, the *charged* tetracoordinate phosphorus effectively excludes a dissociative process, giving a potential opportunity to study steric effects without the complication of mechanism change. Also in contrast to the concerted S_N2 at carbon, halide substitution on this phosphonium system may have two steps: the formation of the pentacoordinate intermediate and its dissociation. We have shown that the stability of this pentacoordinate intermediate is a key determining factor in the rate. In addition, on the basis of substantial amount of computational data on these systems both in the absence and presence of solvent, we provide new insights into the detailed mechanism of this previously overlooked process.

NMR STUDIES

Design and Preparation of Phosphonium Systems. The novel system we devised is shown in Figure 2 (R* = chiral

dx.doi.org/10.1021/ja507433g | J. Am. Chem. Soc. 2014, 136, 16217−16226

group). This simple generic stereochemical system combines epimerization at the phosphorus center with the configurational stability of the carbon stereocenter and gives rise to two pairs of interconverting diastereomers rather than spectroscopically identical enantiomers.[27] We chose *sec*-butyl as the chiral group on phosphorus, it being one of the smallest chiral alkyl substituents. Our results (vide infra) led us to be confident that it is relatively innocent in the reaction. We found that, at ambient temperature, the epimerization of these diastereomeric salts is fast on the NMR time scale, so in most cases only a single peak is observed by ^{31}P NMR. However, at lower temperatures, the exchange was slow enough to allow the individual diastereomers to give distinct signals, and the rates and kinetic barriers could be determined, either by variable-temperature NMR or by exchange spectroscopy (EXSY).

The required salts were formed from the corresponding phosphine oxides (**1a**–**6a**) by treatment with oxalyl chloride or bromide.[24] The oxides in turn were made by standard techniques.[28,29] Chart 1 shows the representative series of

Chart 1. Structures of Halophosphonium Salts and Their Precursor Phosphine Oxides Selected for Study[a]

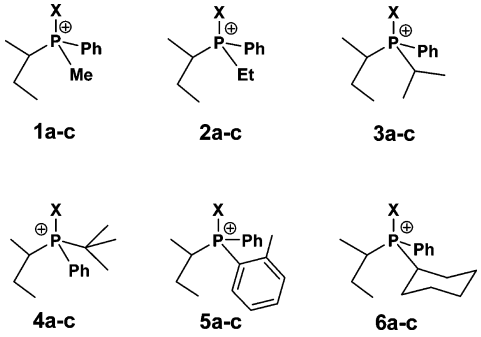

[a]Key: (a) X = O$^-$, no anion; (b) X = Br, anion: Br$^-$; (c) X = Cl, anion: Cl$^-$.

bromo and chloro salts (**1b**–**6b** and **1c**–**6c**) selected for the study. In the series, the phenyl and *sec*-butyl substituents on phosphorus are held constant, and the third substituent is varied to reveal the steric effect of the substituent on the epimerization process.

Observation of Fast Dynamic Processes at Ambient Temperature. As a representative example, the ^{31}P NMR spectra of the salts **2b**/**2c** and oxide **2a** are shown in Figure 3. For the oxide, two signals at δ_P 47.05 and 47.00 ppm corresponding to the two diastereomers are observed. The ^{1}H and ^{13}C spectra of **2a** also show two overlapping sets of peaks, which could be assigned with the aid of two-dimensional COSY, TOCSY, HSQC, and HMBC (see the Supporting Information for details). From their phosphorus NMR shifts, compounds **2b** and **2c** clearly are tetracoordinate phosphonium entities in $CDCl_3$, with the chloro salt **2c** having the slightly higher shift (δ_P 105.3 ppm vs 97.2 ppm). Consistent with this, the α proton on the *sec*-butyl substituent also has a higher shift (δ_H 4.22 ppm vs 4.12 ppm). This is indicative of the more highly polarized nature of the P–Cl bond versus the P–Br bond, consistent with the findings of McAuliffe and co-workers.[25] This polarization may make the phosphorus more susceptible to nucleophilic attack.

Importantly, in the ^{31}P spectra of the salts **2b** and **2c**, only a single sharp peak is observed, and consistent with this, only

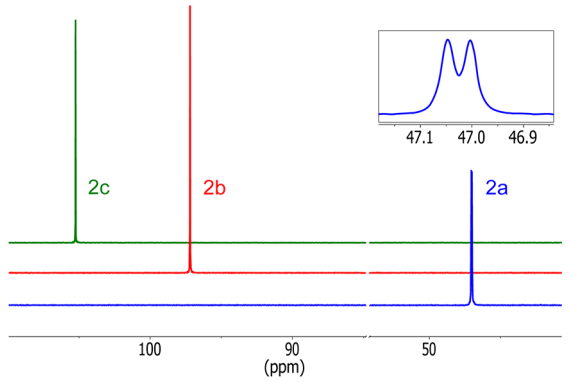

Figure 3. Superimposed ^{31}P NMR spectra of the oxide **2a**, bromide **2b**, and chloride **2c** showing fast equilibration of the two halophosphonium salts (0.05 M, $CDCl_3$, 500 MHz, 30 °C).

single sets of signals are found in the ^{1}H spectra of **2b** and **2c.** This indicates that there is a fast dynamic interconversion of the phosphonium species at this temperature, causing coalescence of the signals. Notably, the diastereotopic protons on the ethyl substituent give one signal corresponding to one carbon, as evidenced by HSQC, as opposed to the four signals corresponding to two distinct carbon atoms in the phosphine oxide **2a**.

Determination of Exchange Barriers. In order to quantify the rate of configurational inversion at phosphorus in halophosphonium salts, we conducted a detailed variable-temperature ^{31}P/^{1}H NMR study, exemplified for the chlorophosphonium salt **3c** in Figures 4 and 5. As the temperature is lowered, the sharp singlet at δ_P 107 ppm in the ^{31}P spectrum of **3c** (Figure 4a, $CDCl_3$ at 30 °C) drifts slightly, broadens, and

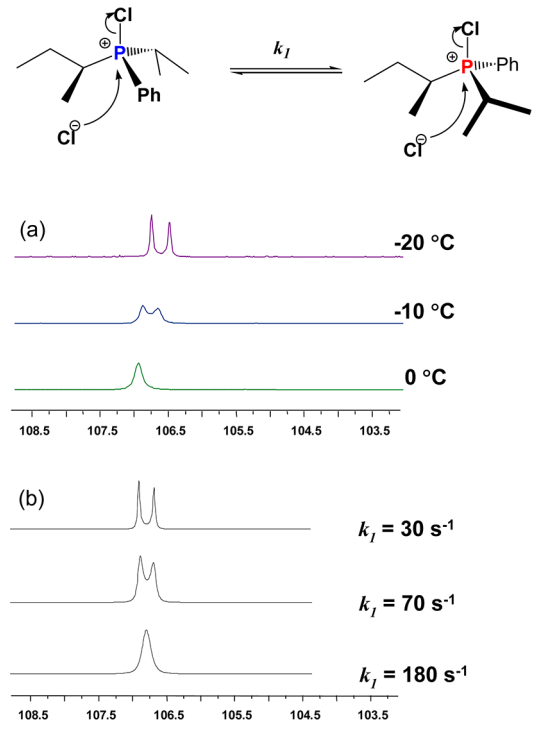

Figure 4. Dynamic NMR study of **3c**: (a) experimental variable temperature ^{31}P NMR profile of **3c** at selected temperatures; (b) dynamic NMR simulation of ^{31}P NMR spectra using variable-exchange rate constants k_1.

dx.doi.org/10.1021/ja507433g | J. Am. Chem. Soc. 2014, 136, 16217–16226

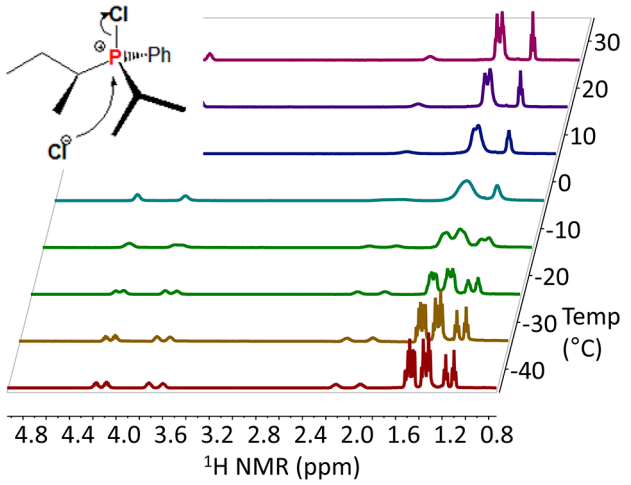

Figure 5. Section of variable-temperature ^{1}H NMR profile of the system **3c** showing decoalescence of peaks in the aliphatic region.

eventually decoalesces to give two distinct signals at δ_P 105.90 and 106.16 ppm with a peak area ratio of 1:1.09. Also shown in Figure 4b is a *Spinworks* DNMR simulation of the ^{31}P spectra of **3c** using the experimental peak separation, 52.5 ± 0.1 Hz, and a variable-exchange rate constant k_1. The fact that line-shape analysis[30] correlates nicely to the authentic ^{31}P NMR data implies that the observed changes in the NMR spectra over a range of temperatures are indicative of a dynamic interconversion of diastereomers. Further Eyring-type analysis of this simulated coalescence data indicated an intercept of 23.4 and a slope of −6588 ± 470 showing that its behavior is close to theoretical for a single-step monomolecular process with activation enthalpy $\Delta H^{\ddagger}$ = +13.1 kcal mol^{-1} and $\Delta S^{\ddagger}$ = 0.7 cal K^{-1} mol^{-1}, giving $\Delta G^{\ddagger}$ of 12.9 ± 0.02 kcal mol^{-1} at 273 K (Supporting Information).

The changes in the ^{1}H NMR spectra of **3c** are also consistent with full decoalescence at the lowest temperature spectra (−50 °C). For example, the triplet in the 30 °C spectrum of **3c** at δ_H 1.13 ppm gives rise to two decoalesced peaks at 1.10 and 1.17 ppm (Figure 5). These signals can be attributed to the protons of the terminal methyl of the *sec*-butyl substituent. The appearance of two sets of signals confirms that the species **3c** is indeed tetrahedral; the pentacoordinate species would not only have a completely different phosphorus NMR spectrum but would also be achiral at phosphorus in its preferred conformation, where both chloro substituents are axial.

Having established that that the inversion of the *P*-configuration in **3c** is fast on the NMR time scale at room temperature but occurs at a measurably slow rate at −30 °C, we were able to find the barrier $\Delta G^{\ddagger}$ to this inversion process directly from the coalescence temperature measurements in chloroform.[31] It is worth noting that part of the rationale for using racemic *sec*-butyl as a chiral substituent was that there would be little, if any, difference in thermodynamic stability of the diastereomers resulting from a *sec*-butyl substituent on a chiral phosphorus center. Had we chosen a larger but, in a sense, "more chiral" substituent that was available as a single enantiomer, the equilibrium could potentially favor one diastereomer. In the case of **3c**, as well as in most other cases, the ratio (dr) of dynamically equilibrating diastereomeric phosphonium cations estimated by ^{31}P and ^{1}H NMR is, within the accuracy of the measurement, close to 1, and this process can reasonably be treated as an equally populated exchange.[31]

Accordingly, knowing the temperature of coalescence (T_c) and the final separation of the peaks in Hz ($\Delta\nu$), we calculated the barrier $\Delta G^{\ddagger}$ to this inversion process at the temperature of coalescence following eq 1 to be 12.9 kcal/mol ±0.1 kcal/mol in good agreement with line-shape analysis results.

$$\frac{\Delta G^{\ddagger}}{RT_c} = \ln\left(\frac{T_c k_B \sqrt{2}}{\pi \Delta\nu h}\right) \quad (1)$$

The inversion barriers found for chloro- and bromophosphonium salts derived from the oxides **2**, **3**, **5**, and **6** are summarized in Table 1 (see Table S1 of the Supporting Information for coalescence temperatures). The interconversion of the chloride **1c** bearing the smallest alkyl substituent CH_3 was too fast, even at −80 °C, on the NMR time scale to allow for the determination of the exchange barrier which is estimated therefore as <9 kcal mol^{-1}. At the other extreme, in the BPS **4b** with bulky *t*-Bu group, no coalescence was observed up to 50 °C and ^{1}H EXSY (vide infra) was used to determine the rate of interconversion and the exchange barrier which, in this case, is 19.2 kcal mol^{-1}. Interestingly, only in **4b** and **4c** did the rate and stability of the two diastereomers differ significantly and result in an unequal mixture. The ratio in the case of **4c** at 223 K is 1:1.6, giving a difference in energy of 0.21 kcal/mol, while a ratio of 1:1.37 at 303 K was found in **4b** indicating a difference in stability of 0.19 kcal mol^{-1}.

Table 1. Epimerization Barriers and Corresponding Exchange Rates in Halophosphonium Salts 1−6[a]

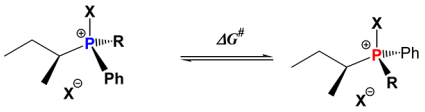

	$\Delta G^{\ddagger}$ (kcal mol^{-1})		k_1 at 0 °C (s^{-1})	
R	X = Cl	X = Br	X = Cl	X = Br
Me	<9[b]	11.7	>3.6 × 10^5	2.5 × 10^3
Et	11.3	13.2	5.3 × 10^3	1.6 × 10^2
i-Pr	12.9	14.6	2.8 × 10^2	1.2 × 10^1
t-Bu	15.1	19.2[c]	4.8 × 10^0	2.5 × 10^{-3}
o-Tol	11.7	14.1	2.5 × 10^3	3.0 × 10^1
c-Hex	12.5	14.9	5.8 × 10^2	7.0 × 10^0

[a]Solutions in $CDCl_3$, *c* = 0.05 M, rates from VT-NMR experiments, errors estimated as ±0.2 kcal/mol based on 3 K temperature variation in the coalescence; [b]Upper limit due to experimentally available temperature range; [c]Barrier ascertained by 2D-exchange spectroscopy (see text).

Two important findings regarding the rates of pseudodegenerate nucleophilic displacement can be discerned from analysis of the results presented in Table 1. First, the reactivity of bromides is significantly and consistently lower than the corresponding chlorides, with energy barriers to the inversion higher by ca. 2 kcal mol^{-1}. This observation is perhaps not completely unexpected since, although bromide is often regarded as better leaving group and better nucleophile, its nucleophilicity in aprotic media is lower than the more densely charged chloride.[32]

Second, much like S_N2 at carbon, the size of substituents has a very significant effect on rate, with large groups inhibiting the approach of the nucleophile. Introduction of each additional carbon increases the barrier in the sequence Me < Et < *i*-Pr < *t*-Bu, adding 1.5−2 kcal mol^{-1} each time. Conversely,

dx.doi.org/10.1021/ja507433g | J. Am. Chem. Soc. 2014, 136, 16217−16226

introduction of an additional aromatic *o*-tolyl group, as in **5b/c**, does not lead to significant variation of the barrier when compared to cyclohexyl analogues **6** as well as similarly branched *i*-Pr systems **3**. Most interesting is that the trends in reactivity of CPS and BPS depart from that of tetracoordinate carbon because increasing the steric demand or adding aromatic groups at the positively charged phosphorus center does not induce a dissociative S_N1-type mechanism, the formation of phosphonium dication not being feasible. Instead, the barrier to nucleophilic attack continues to increase when more sterically demanding groups are introduced. This effectively allows a true estimate of the steric effect of *t*-Bu compared to that of *i*-Pr adjacent to a tetrahedral reaction center.

It could be argued that the best phosphorus analogue for carbon is phosphonium, and so we were anxious to find a suitable comparison. The best available carbon comparison for our results is with substitution at primary alkyl bromide[33] (Table 2). It can be seen immediately that steric effects at

Table 2. Effect of Steric Hindrance on Bromide Exchange at Carbon and Phosphorus Centers at 298 K

R	$RCH_2Br + Br^-$ rel rate[a]	$R^sBuPhP^+Br + Br^-$ rel rate[b]
t-Bu	1	1
i-Pr	2.2×10^3	2.3×10^3
Et	4.2×10^4	2.5×10^4
Me	6.7×10^4	3.1×10^5

[a]From ref 33, measurements at 25 °C. [b]from experimentally determined barriers shown in Table 1. Rates calculated for 25 °C.

quaternary phosphonium are approximately comparable to those at primary carbon at least in this case. This may seem surprising but we note that it may be the result of two opposing effects: the shorter C-C bond should render carbon more sensitive to steric effects but the other substituents at carbon in this case are much less bulky hydrogens.

Reaction Mechanism and Order. We have previously reported[24] that certain chlorophosphonium salts in the crystalline state contain solvent-separated ion pairs, shown schematically in Figure 6b. If this structure persists in solution,

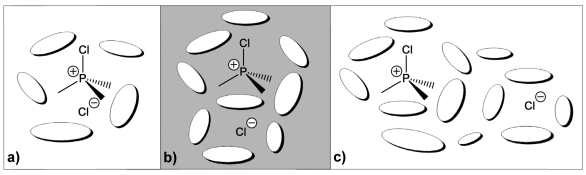

Figure 6. Possible interactions between ionic components of halophosphonium salts in solution: (a) tight ion pairs; (b) solvent-separated ion pairs; (c) fully dissociated ions.

individual halide anions will proceed to attack their associated phosphonium cations, regardless of concentration, resulting in first-order kinetics for this associative process. Similarly, first-order kinetics can be expected in the presence of fully solvated tight ion pairs shown in Figure 6a. However, if the salt exists as fully solvated dissociated ions (Figure 6c), where a chloride ion can attack any nearby phosphonium, second-order kinetics can be expected.

For the determination, we chose the more hindered chlorophosphonium salt **4c**, as this was considered most likely to exist as a fully dissociated species in solution such that any concentration effects might be most marked. Also, being the more soluble in chloroform, the chlorophosphonium salts are more suitable than the bromophosphonium salts for experiments across a wider range of concentrations. The ^1H NMR spectrum of **4c** at 30 °C is shown in Figure 7. The considerable

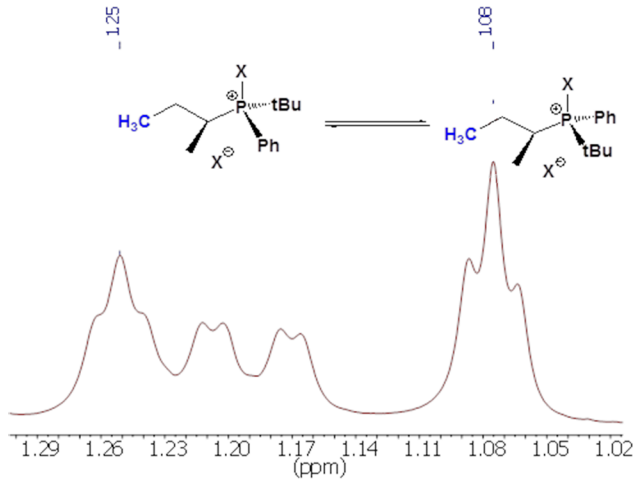

Figure 7. ^1H NMR spectrum of **4c** at 30 °C with broadening indicative of an exchange process. The triplet signals correspond to the CH_3 groups γ to the phosphorus atom.

broadening of the signals observed in this case suggests that a relatively slow dynamic exchange process takes place at this temperature. Its rate, estimated by VT-NMR (Table 1), is within the range that could be more conveniently and accurately monitored by 2D exchange spectroscopy, EXSY. In EXSY an irradiating pulse changes the state of a particular hydrogen in a molecule. This is followed by a mixing time, T_m, after which the proton may find itself in a new chemical environment due to some exchange process or conformational change in the molecule. An analyzing pulse is then applied, and the proportion of hydrogens that have changed environment during the mixing time can be measured by the integration of cross peaks vs diagonal peaks in the spectrum. The mixing time can be varied and conversion after different periods of time can be determined. When performed on a relatively slow system, EXSY also allows measurement of the reaction progress at varying time intervals and construction of a kinetic profile from a single concentration.[34] Thus, for example, the triplet signals of the methyl groups shown at 1.08 and 1.25 ppm in Figure 7 correspond to the two different diastereomeric forms of **4c** and have different chemical environments. While the signals are appreciably broadened, they are still sufficiently resolved for a clear EXSY spectrum to be obtained (Figure 8).

When EXSY measurements of **4c** were carried out across a range of concentrations, no change in the epimerization rate was observed. Shown in Figure 8 are three sample EXSY spectra of **4c** (T_m = 10 ms) taken at three different concentrations. Importantly, the integration of the cross-peak corresponding to chemical exchange between two diastereomeric forms of **4c** remains the same within the precision of this experiment. This indicates that the salt **4c** exists as either a tight ion pair or a solvent-separated ion pair in solution (see Figure 6). It is more likely that a solvent-separated ion pair is present, as has been observed in crystal structures of phosphonium salts,[25] whereby the anion is bound by medium-range electrostatic forces.

dx.doi.org/10.1021/ja507433g | J. Am. Chem. Soc. 2014, 136, 16217−16226

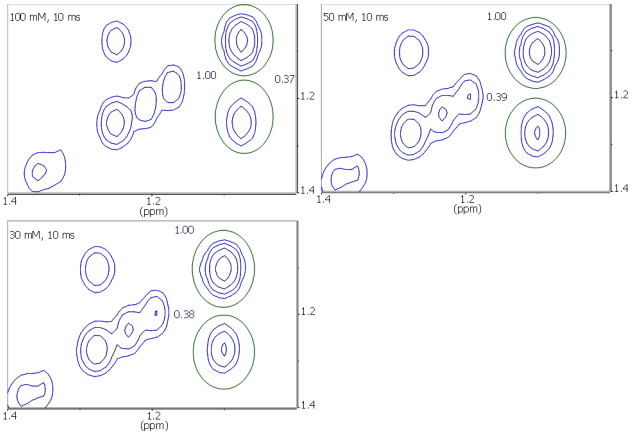

Figure 8. EXSY spectra of **4c** show no change in rate of epimerization with varying concentration (from 100 mM to 30 mM) and constant mixing time (10 ms). The rate of epimerization can be calculated from the volume of the diagonal peaks and the volume of the cross peaks. The volumes integrated are denoted by the green ovals.

Comparison with Carbon Chemistry. On the one hand, substitution at phosphonium is, perhaps superficially, analogous to S_N2 in that it is an associative reaction of a tetracoordinate entity and a nucleophile followed by the formation of a pentacoordinate intermediate and the departure of a leaving group. However, in our S_N process, the tetracoordinate species is charged and the pentacoordinate species is neutral, the opposite of the S_N2 process at carbon. As we will show in the computational section below, we have good reason to believe that the symmetrical, or pseudosymmetrical, pentacoordinate R_3PX_2 species is a true intermediate, with two associated pentacoordinate transition states in which one of the two P−X bonds is very significantly elongated. On the other hand, the observed reaction kinetics demonstrate that the epimerization of phosphonium salts is a first order process, akin to S_N1. The dissimilarity is that, in our system, the rate is only dependent on one reactant for a different reason: the nucleophile and substrate exist as an ion pair (tight or solvent-separated), so concentration does not affect the probability of an individual reaction event.

A solvent study would be desirable for further insight into the mechanism of this process. Unlike carbon chemistry, a fully associative mechanism with a true intermediate is possible at phosphorus. In addition, the tetracoordinate species studied here are charged but their reaction proceeds through a neutral intermediate (vide infra) and transition states, making the reaction in less polar solvents more feasible. This is in contrast to most carbon-centered reactions in which neutral reagents react through charged transition states, facilitated by polar solvents. Both deuterated benzene and carbon tetrachloride were considered as alternative nonpolar solvents (McAuliffe and co-workers had previously described the properties of halophosphonium salts in benzene[25]). Unfortunately, owing to the poor solubility of the halophosphonium salts, it was not possible to carry out variable-temperature NMR or EXSY in those solvents. In the meantime, we have done thorough computational investigations (next section) of the reaction profiles in different solvents in pursuit of an accurate mechanistic model. According to our computational studies, nonpolar solvents lower the barrier to this epimerization substantially by stabilizing the pentacoordinate, neutral intermediate relative to the tetracoordinate species.

COMPUTATIONAL RESULTS

We wished to use a computational methodology that would allow us to directly analyze the reactivity of compounds **1**−**6b**,**c**. We have used three computational approaches (Chart 2) which taken together provide the required analysis for a reasonable effort in terms of calculation time and cost. In the most basic "single point" approach, the energy of a proposed, and arbitrarily symmetrical, pentacoordinate intermediate is compared to the energy of the "ground state" while the shape of the energy profile remains unknown (Chart 2, a); in the "single-constraint" method a moderate number of points along the reaction coordinate are calculated creating an energy profile (Chart 2, b). Finally, the full three-dimensional PES is built by calculating a large set of points in a double-constraint approach shown as 2D-projecton (Chart 2, c). The computational cost at this last stage is increased by 2 orders of magnitude.

Chart 2. Three Computational Approximations of Degenerate Reaction Energy Barrier: (a) Single Point; (b) Single Constraint Profile; (c) Double-Constraint 3D-PES (Top View)

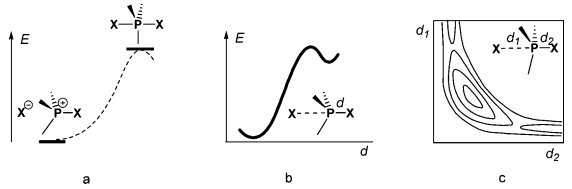

For our calculations, we used density functional theory (DFT) calculations with the B3LYP 6-31G* basis set. Since very significant changes of reaction PES in phosphorus chemistry are known to be associated with solvation (see Figure 1),[15,16] the simplest halophosphonium derivatives Me_3PCl_2 (**8a**) and Me_3PBr_2 (**8b**) were treated in vacuo and in solution using an SM8 model.[35] This was followed by computation of detailed PES for the fully degenerate model exchange systems in vacuo and in a polar solvent. Finally, the calculations were extended to all sample halophosphonium systems **1**−**6** showing a very reasonable conformity with experiment.

Single-Point Approximation. For symmetrical models **8** the calculated equilibrium geometries of both **8b** and **8c** in vacuo corresponded to the pentacoordinate diaxial structure, whereas in DCM, tight ion pairs were more stable. Their ionic character is backed by calculated interatomic distances $d_{(P-Cl)}$ = 3.85 Å and $d_{(P-Br)}$ = 4.11 Å and also the negative Mulliken charges of distal halides (greater than −0.9). In the following step, the calculations of energy *without* geometry optimization were repeated for the pentacoordinate diaxial species in DCM and for ion pairs in vacuo as shown in Figure 9 (all energies are referenced to the ionic forms of **8b** and **8c** in vacuo).

Analysis of the data in Figure 9 indicates that, in vacuo, the dichloride **8c** has a stronger, by ca. 3 kcal mol^{-1}, preference for the pentacoordinate form than the dibromide **8b**. However, the presence of a polar solvent leads to a very significant, up to 30 kcal mol^{-1}, stabilization of the ionic forms. The solvation effects are stronger for the ionic bromide **8b** putting it *lower* than the ionic chloride **8c**. Consequently, the energy required to invert the tetrahedral bromide **8b** via the pentacoordinate intermediate is ca. 2.5 kcal mol^{-1} *higher* than the chloride **8c**. This finding is in excellent agreement with experimental observation (see Table 2) that energy barriers to pseudodegenerate exchange of bromides **1b**−**6b** are generally ca. 2 kcal mol^{-1} higher as compared to chlorides.

Single-Constraint Profile. A single-constraint approach was applied to model **8a** in such a fashion that one of the P−Cl distances was constrained and the system was allowed to reach a new equilibrium geometry. Since the calculated distance $d_{(PCl)}$ for the equilibrium geometry in vacuo is 2.31 Å and in DCM it reached 3.85 Å, the energy plots for Me_3PCl_2 were performed in the $d_{(PCl)}$ range 2.2−3.9 Å with a geometric resolution of 0.05 Å. The resulting energy

dx.doi.org/10.1021/ja507433g | J. Am. Chem. Soc. 2014, 136, 16217−16226

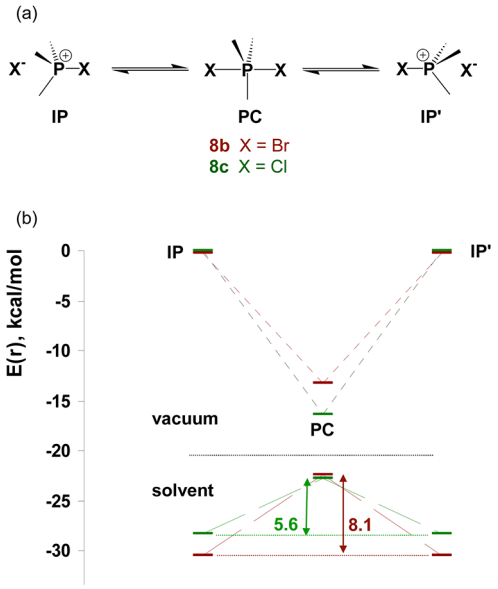

Figure 9. (a) Degenerate interconversion of ion pairs (IP) via pentacoordinate intermediate Me_3PX_2 in the model system **8**; (b) calculated energies of these species in vacuo and in polar solvent (DCM) showing higher relative energy of pentacoordinate dibromide (brown) than chloride (green).

profiles in vacuo, toluene, DCM, and chloroform appear as shown in Figure 10.

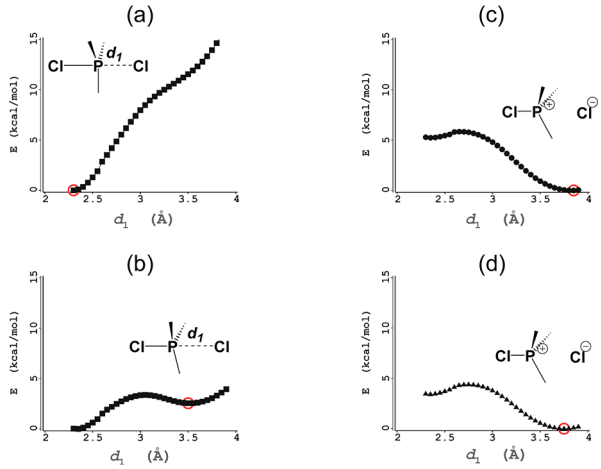

Figure 10. Single-coordinate energy profiles of the system **8a**: (a) in vacuo, diaxial pentacoordinate species shown is most stable; (b) in toluene, a second local minimum corresponds to a compact ion pair; (c) in DCM and (d) chloroform. The energy minimum corresponds to an unsymmetrical pentacoordinate state as shown.

Clearly, the calculated energy profiles in vacuo and toluene (Figures 10a/10b) are very different, both from each other and from DCM or chloroform (Figure 10c,d). In vacuo, as discussed above, the pentacoordinate form is more stable, and dissociation of chloride anion is forbidden energetically. The energy profile shows a monotonic rise up to $d_{(PCl)}$ = 3.9 Å (the system requires ca. 46 kcal mol^{-1} for complete dissociation). In toluene, however, a second local energy minimum is clearly visible. It lies 2.6 kcal mol^{-1} above the pentacoordinate form and corresponds to a somewhat compressed ion-pair geometry whereby $d_{(P-Cl)}$ = 3.5 Å and partial charge on Cl is −0.84. In the more polar chloroform the relative energy of ion pairs is lower, making the pentacoordinate form unstable. Similarly, in DCM (dielectric constant 9) the pentacoordinate form is further destabilized: the fully symmetrical system is 5.2 kcal mol^{-1} higher than ion pairs but it occupies a 0.6 kcal mol^{-1} deep local energy minimum. This means that the degenerate interconversion of model chlorophosphonium ion pairs **8a** will have to overcome a *double-maximum* energy barrier (compare Figure 1a). The calculated height of this barrier is 5.8 kcal mol^{-1} as shown in Figure 10c. Importantly, this observation of a local energy minimum corresponding to the symmetrical pentacoordinate intermediate in medium-polar solvents is in excellent agreement with previous computational results showing a double-maximum energy profile for substitution reaction at tetracoordinate phosphorus.[16] Our findings demonstrate that single-point approximation of the energy barrier to interconversion of halophosphonium halides (see Figure 9) gives an estimate which is inevitably *lower* than calculated from detailed (the resolution has to be at least 0.1 Å) energy profiles shown in Figure 10c,d.

Double-Constraint Calculations: More O'Ferrall–Jencks Plot. In our view, the most fitting way to discuss the energetics of the model system is through the three-dimensional PES best known as the More O'Ferrall–Jencks plot,[36] a two-dimensional projection of the PES. This representation, while not claiming mathematical precision, gives a tangible sense of the progress of the reaction, while taking a number of variables into consideration. For example, in carbon chemistry, it has been used to describe the continuum of reactivity from S_N1 to S_N2 in nucleophilic substitution at carbon. Such plots can show how the change from a concerted mechanism to a dissociative mechanism is facilitated by increasing the substitution on the central carbon atom. However, our model reaction system, Me_3PX_2, likely occupies the opposite far corner of such a plot, as dissociation from the positively charged phosphorus is impossible, but both concerted and fully associative mechanisms are feasible. Furthermore, computational studies of our system indicate that as the reaction moves closer to a fully associative mechanism involving a stable pentacoordinate intermediate, two barriers appear in the reaction coordinate. At the extreme end of this trend, in vacuo, the tetracoordinate salts are the least stable species, and the pentacoordinate "intermediate" becomes the predominant form. Unfortunately, despite the fact that detailed three-dimensional PES represent significant advantages, very few such systems have been investigated computationally, and little, if anything, is known about reactions at tetracoordinate phosphorus.[37]

In this work, for the first time, we applied a double-variable-constraint approach to a phosphonium system, Me_3PCl_2. In these computations, both P–Cl distances d_1 and d_2 were constrained independently, and the system was allowed to reach equilibrium geometry. The resulting energy profiles in vacuo with a geometric resolution of 0.1 Å and in DCM with a geometric resolution 0.05 Å appear as Figures 11 and 12, respectively. In excellent agreement with

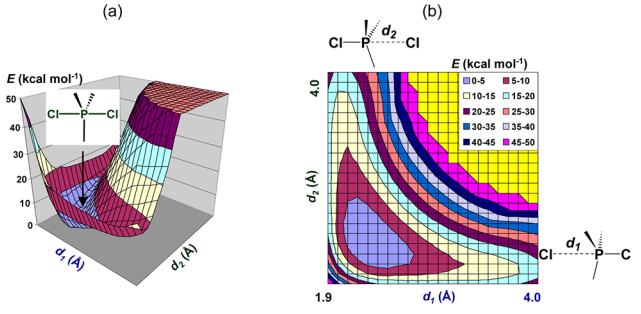

Figure 11. Calculated (0.1 Å resolution) 3D energy diagram of Me_3PCl_2 **8c** in vacuo: (a) side view; (b) More O'Ferrall plot view.

the single-constraint results (Figure 10), as expected, the PES of system **8c** in vacuo exhibits a global minimum corresponding to the symmetrical pentacoordinate species as shown in Figure 11a. This area of low energy can also be clearly seen on the More O'Ferrall plot (Figure 11b) as a relatively broad minimum centered around 2.3 Å in both dimensions.

dx.doi.org/10.1021/ja507433g | J. Am. Chem. Soc. 2014, 136, 16217–16226

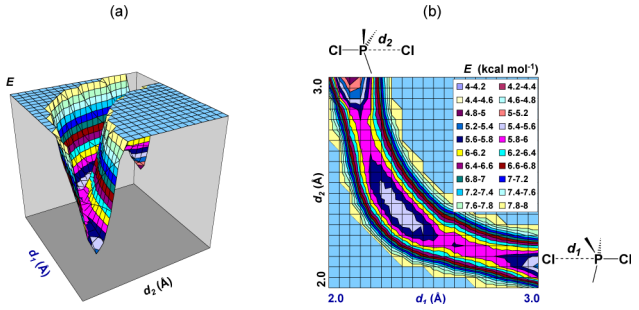

Figure 12. Calculated (0.05 Å resolution) energy diagrams of Me_3PCl_2 in DCM: (a) side view; (b) More O'Ferrall plot view.

Calculations of the PES in polar solvent (DCM) were done in the critical 3−4 Å constraint range with enhanced resolution of 0.05 Å in each dimension d_1 and d_2. The results (Figure 12a) indicate a very defined reaction pathway for the degenerate interconversion of ion-pairs, which can be seen as a narrow, gully like energy profile. Most significantly the More O'Ferrall representation (Figure 12b) clearly shows two defined separate "gaps" on the energy profile in agreement with our previous single-coordinate reaction energy diagrams (Figures 1 and 10) and other published results.[16] The two gaps are separated by a local energy minimum ca. 0.5 kcal mol^{-1} deep. Viewed as a whole, the plot represents an associative-type mechanism as the reaction pathway lies far from the diagonal whereby the changes of both variable distances d_1 and d_2 are simultaneous. On the basis of our detailed calculations, it can be concluded that the substitution of halide at the phosphorus occurs as a quasiconcerted nucleophilic process characterized by formation of a very short-lived pentacoordinate intermediate and accompanied by Walden-type inversion of the *P*-configuration.

In this context, with respect to the stereochemistry, it is worth considering possible pseudorotation in a pentacoordinate intermediate. Our calculations indicate that the energy of an axial−equatorial configuration of phosphonium dihalides (see Figure 1b) is higher by 15−16 kcal/mol than the diaxial species due to the high apicophilicity of halogens. For our systems, this indicates that pseudorotation is not the mode of inversion. This is consistent with the negligible barriers to Walden inversion found by Bickelhaupt and co-workers in the phosphoryl series,[7] which adds weight to our assertion that the inversion occurs through backside nucleophilic attack rather than pseudorotation.

Computational Estimation of Energy Barriers. With an understanding of the attributes of our different calculational approaches, we were in a position to study the more complex systems **1b**−**6b** and **1c**−**6c** (see Chart 1). In principle, this should be done at one- and two-dimensional PES surface levels. However, since both the tetra- and pentacoordinate species involved typically possess a number of rotational degrees of freedom, it is important to take into account various conformations of these systems. Therefore, the working out of detailed energy profiles at one- and two-dimensional levels would represent a rather demanding computational task, beyond the scope of this paper. Instead, we applied the single-point approach utilized for the model systems **8b** and **8c** and which gave the fairly reliable results shown in Figure 9. For each given dihalide, the most stable conformer of the pentacoordinate diaxial system in vacuo was identified as a first step. Similarly, in solution, where ion pairs are more stable, the calculations were done to find the most stable conformer of the respective halophosphonium halide ion pairs. Then the calculations were carried out for the pentacoordinate diaxial species in solvent *without* geometry optimization (full geometry optimization would lead to ionic tetracoordinate species), and the resulting energy was compared to the solvated ion pairs. These single-point computational results on the relative stabilities of the pentacoordinate and tetracoordinate forms of our chloro- and bromophosphonium salts **1**−**6** in DCM are given in the Supporting Information (Table 3).

To our delight, the computational results closely followed the experimental trends. First, the bromophosphonium salts were calculated to have higher barriers to epimerization than the chlorophosphonium salts. Second, the steric effects observed experimentally were almost identically reciprocated in the computational results. Graphically, these findings can be represented by the reasonably linear correlation between experimental barrier and computationally estimated relative intermediate energy shown in Figure 13.

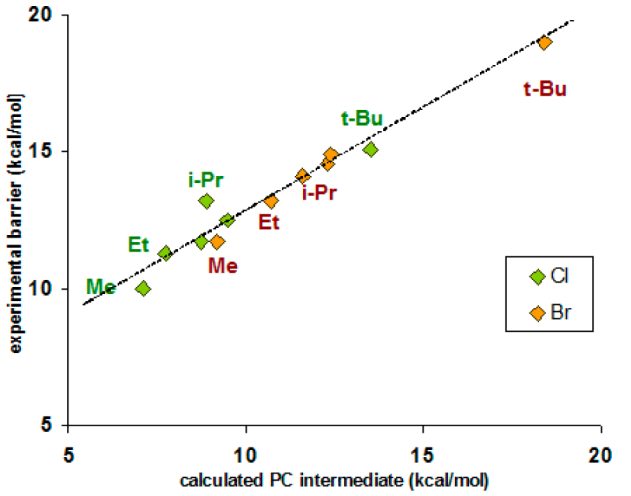

Figure 13. Comparison of calculated energy of pentacoordinate intermediate and experimentally found barriers to epimerization showing reasonably good linear correlation.

It is notable that, in most cases, the calculated energy of formation of the pseudosymmetrical pentacoordinate intermediates was approximately 3−4 kcal mol^{-1} lower than the experimentally determined barriers. This discrepancy could be due to a number of factors. First of all, as we have demonstrated for the model system **8c** (see Figure 10), the symmetrical pentacoordinate form is not the maximum on the reaction energy profile and its energy compared to the tetracoordinate species should be lower than the energy of the transition state. Moreover, if an unsymmetrical pentacoordinate species, e.g., **2c**, is a true intermediate, it may have *two* different transition states associated with it, which would be higher in energy than the pentacoordinate form. Since the transition states are not symmetrical the pentacoordinate species occupies a nonsymmetrical local energy minimum. This would result in a distinct double-crested reaction energy profile as was proposed by Bickelhaupt and co-workers for their related process.[7]

A second reason for the discrepancy between experimental and calculated barriers is that the experimentally determined barrier is a measure of the Gibbs free activation energy of the system. The calculated energy difference between pentacoordinate and tetracoordinate forms does not account for entropy; entropy would be expected to contribute to raising the free energy of the transition state of this system. Third, our present approach to solvation cannot be entirely accurate since we have recently shown[24] that the halophosphonium salts are prone to formation of solvent-separated ion pairs (SSIP), which can be observed in the solid state. If similar solvent-separated ionic structures persist in solution, their energy is possibly lower than calculated for contact ion pairs, leading to a further increase of the barrier, owing to a more stable ground state. A higher level molecular dynamics model would be required to account for this solvation effect, which should also take into account specific solvent−ion interactions.

As noted in the Computational Results, the steric effects on nucleophilic attack at phosphonium center are comparable to those at carbon centers despite the longer P−C and P−X bonds. The model systems RMe_2PCl_2, where R = Me, Et, ^{t}Bu, were employed to examine this effect. Indeed, the reaction profile for Me_3PCl_2 had a pronounced

dx.doi.org/10.1021/ja507433g | J. Am. Chem. Soc. 2014, 136, 16217−16226

double-crested reaction profile denoting a true pentacoordinate intermediate; $EtMe_2PCl_2$ had a shallow local minimum in its double-crested profile, whereas *t*-$BuMe_2PCl_2$ had a single crest and the pentacoordinate form became a transition state. Interestingly, the more sterically encumbered systems have *wider* and less steep reaction energy profiles (see the Supporting Information, Figure 21) owing to the greater distance between anion and cation. This is consistent with the analysis of Frenking and co-workers, specifically with respect to the weakening of the axial bonds.[6a]

CONCLUSIONS

In this study we have been able, for the first time, to determine experimentally the rates of degenerate nucleophilic substitution reactions at a tetracoordinate phosphorus center and established the general trends in the substrate reactivity. This was achieved by a novel experimental design that has wider potential application. Further, we have also designed a viable computational approach to this system, the results of which accurately reflected our experimental findings, bolstering our confidence in the finer mechanistic details it yielded.

The key finding is that diastereomeric halophosphonium salts exhibit two sets of signals in the NMR spectrum at low temperature and one set at room temperature. On the basis of this finding, the rates of epimerization at the phosphorus center and the respective energy barriers have been quantified by using a combination of variable-temperature NMR and EXSY techniques, across 8 orders of magnitude in terms of reactivity.

We were able to quantify a dependence of the rate on the size of the substituent attached to phosphorus, analogous to trends in substitution processes at other elements. The rate varies over 5 orders of magnitude depending on the substituents. The importance of steric effects is proof of an associative or concerted mechanism via a pentacoordinate transition state or intermediate, bearing two axial halogens. In contrast to carbon, the mechanism of substitution cannot become dissociative with increasing substituent bulk, so that the measured steric effects of individual substituents are potentially transferrable parameters for other processes.

The degree of variation of steric effect along the sequence Me < Et < ^{i}Pr < ^{t}Bu was found to be the same for phosphorus as for carbon in the best available comparison. We speculate that this will be replicated for other main group elements.

The barriers to inversion in chlorophosphonium salts are lower than those in the corresponding bromophosphonium salts by up to 2 kcal mol^{-1}. Our computational results suggest that, in a polar solvent medium, this difference is due to the easier accessibility of pentacoordinate dichlorophosphoranes when compared to analogous dibromophosphoranes.

By varying their concentration, we have found that the halophosphonium salts exist as tight or solvent-separated ion pairs in solution leading to first-order kinetics. This diverges from the analogous substitution process at carbon and thus can be better described as S_N1_{asc}.

Three-dimensional reaction potential energy profiles (More O'Ferrall–Jencks plots) indicated a relatively shallow potential well corresponding to the trigonal bipyramid intermediate flanked by two transition states.

Our findings have significantly improved the understanding of reaction mechanisms involving penta- and tetracoordinate phosphorus and their relationships to other elements.

ASSOCIATED CONTENT

Supporting Information

Characterization of compounds, VT-NMR arrayed spectra and analysis, EXSY spectra and analysis, computational details, and absolute energies for geometry optimized molecules. This material is available free of charge via the Internet at http://pubs.acs.org.

AUTHOR INFORMATION

Corresponding Author

declan.gilheany@ucd

Funding

This work was supported by Science Foundation Ireland through Principal Investigator Grant No. 09/IN.1/B2627.

Notes

The authors declare no competing financial interest.

ACKNOWLEDGMENTS

We are grateful to the UCD Centre for Synthesis and Chemical Biology (CSCB) and the UCD School of Chemistry and Chemical Biology for access to their extensive analysis facilities and to Science Foundation Ireland for funding.

DEDICATION

This work is dedicated to the memory of Professor Rory More O'Ferrall (1937–2012) whose pioneering work on three-dimensional reaction energy profiles in the early 1970s contributed to the inspiration for this mechanistic study.

REFERENCES

(1) (a) Hughes, E. D.; Ingold, C. K.; Martin, R. J. L.; Meigh, D. F. *Nature* **1950**, *166*, 679–680. (b) Ingold, C. K. *Structure and Mechanism in Organic Chemistry*, 2nd ed., Cornell University: London, 1969: Chapter VII.

(2) Anslyn, E. V.; Dougherty, D. A. *Modern Physical Organic Chemistry*; University Science Books: Sausalito, 2006; p 637.

(3) Clayden, J. P., Greeves, N., Warren, S., Wothers, P. D. *Organic Chemistry*; Oxford University Press, Oxford, 2006; p 411.

(4) (a) Krause, N.; Gerold, A. *Angew. Chem., Int. Ed.* **1997**, *36*, 186–204. (b) Lee, I. *Chem. Soc. Rev.* **1995**, *24*, 223–229. (c) Sneen, R. A. *Acc. Chem. Res.* **1973**, *6*, 46–53.

(5) Manikandan, P.; Zhang, J.; Hase, W. L. *J. Phys. Chem. A* **2012**, *116*, 3061–3080 and references cited therein.

(6) Somewhat contentiously: (a) Fernandez, I.; Frenking, G.; Uggerud, E. *Chem.—Eur. J.* **2009**, *15*, 2166–2175. (b) van Zeist, W.-J.; Bickelhaupt, F. M. *Chem.—Eur. J.* **2010**, *16*, 5538–5541. (c) Fernandez, I.; Frenking, G.; Uggerud, E. *Chem.—Eur. J.* **2010**, *16*, 5542–5543. (d) Schwarz, W. H. E.; Schmidbaur, H. *Chem.—Eur. J.* **2012**, *18*, 4470–4479. (e) Pinter, B.; Fievez, T.; Bickelhaupt, F. M.; Geerlings, P.; De Proft, F. *Phys. Chem. Chem. Phys.* **2012**, *14*, 9846–9854.

(7) van Bochove, M. A.; Bickelhaupt, F. M. *Eur. J. Org. Chem.* **2008**, *4*, 649–654.

(8) (a) Wu, C.-H.; Galabov, B.; Wu, J. I-C.; Ilieva, S.; Schleyer, P. v. R.; Allen, W. D. *J. Am. Chem. Soc.* **2014**, *136*, 3118–3126. (b) Buck, H. M. *Int. J. Quant.* **2011**, *111*, 2242–2250.

(9) (a) Bergin, E.; O'Connor, C. T.; Robinson, S. B.; McGarrigle, E. M.; O'Mahony, C. P.; Gilheany, D. G. *J. Am. Chem. Soc.* **2007**, *129*, 9566–9567. (b) Rajendran, K. V.; Kennedy, L.; Gilheany, D. G. *Eur. J. Org. Chem.* **2010**, 5642–5649. (c) Rajendran, K. V.; Kudavalli, J. S.; Dunne, K. S.; Gilheany, D. G. *Eur. J. Org. Chem.* **2012**, 2720–2723. (d) Rajendran, K. V.; Gilheany, D. G. *Chem. Commun.* **2012**, *48*, 10040–1042. (e) Carr, D. J.; Kudavalli, J. S.; Dunne, K. S.; Gilheany, D. G. *J. Org. Chem.* **2013**, *78*, 10500–10505. (f) Nikitin, K.; Rajendran,

K. V.; Müller-Bunz, H.; Gilheany, D. G. *Angew. Chem., Int. Ed.* **2014**, *53*, 1906−1909.
(10) Bürgi, H.-B.; Shklover, V. *Reaction Paths for Nucleophilic Substitution (S_N2) Reactions, in Structure Correlation*; Bürgi, H.-B., Dunitz, J. D., Eds.; Wiley−VCH: Weinheim, Germany, 2008;Vol. *1*, DOI: 10.1002/9783527616091.ch07.
(11) Holmes, R. R. *Chem. Rev.* **1990**, *90*, 17−31.
(12) (a) Corriu, R. J. P.; Guerin, C. *J. Organomet. Chem.* **1980**, *198*, 231−320. (b) Corriu, R. J. P.; Guerin, C. *Adv. Organomet. Chem.* **1982**, *20*, 265−312.
(13) Berry, R. S. *J. Phys. Chem.* **1960**, *32*, 933−938.
(14) Deiters, J. A.; Holmes, R. *J. Am. Chem. Soc.* **1987**, *109*, 1686−1892.
(15) van Bochove, M. A.; Swart, M.; Bickelhaupt, F. M. *J. Am. Chem. Soc.* **2006**, *128*, 10738−10744.
(16) (a) van Bochove, M. A.; Swart, M.; Bickelhaupt, F. M. *Phys. Chem. Chem. Phys.* **2009**, *11*, 259−267. (b) van Bochove, M. A.; Swart, M.; Bickelhaupt, F. M. *ChemPhysChem* **2007**, *8*, 2452−2463.
(17) Muetterties, E. L. *Acc. Chem. Res.* **1970**, *3*, 266.
(18) (a) Bone, S. A.; Trippett, S.; Whittle, P. J. *J. Chem. Soc., Perkin Trans. 1* **1977**, 437−438. (b) Trippett, S. *Pure Appl. Chem.* **1974**, *40*, 595−605.
(19) (a) Granoth, I.; Segall, Y.; Leader, H. *J. Chem. Soc., Chem. Commun.* **1976**, 74−75. (b) Buono, G.; Llinas, J. R. *J. Am. Chem. Soc.* **1981**, *103*, 4532−4540.
(20) Holmes, R. R. *Pentacoordinated Phosphorus*; ACS Monograph 175; American Chemical Society: Washington, DC, 1980; Vols. *1* and *2*.
(21) Appel, R.; Halstenberg, M. In *Organophosphorus Reagents in Organic Synthesis*; Cadogen, J. I., Ed.; Academic Press: London, 1979; Chapter 9.
(22) (a) Byrne, P. A.; Rajendran, K. V.; Muldoon, J.; Gilheany, D. G. *Org. Biomol. Chem.* **2012**, *10*, 3531. (b) Rajendran, K. V.; Carr, D. J.; Gilheany, D. G. *Tetrahedron Lett.* **2011**, *52*, 7113. (c) Rajendran, K. V.; Gilheany, D. G. *Chem. Commun.* **2012**, *48*, 817. (d) Kenny, N. P.; Rajendran, K. V.; Jennings, E. V.; Gilheany, D. G. *Chem.—Eur. J.* **2013**, *19*, 14210−14214. (e) Rajendran, K. V.; Kennedy, L.; O' Connor, C. T.; Bergin, E.; Gilheany, D. G. *Tetrahedron Lett.* **2013**, *54*, 7009−7012.
(23) (a) Denton, R. M.; An, J.; Adeniran, B. *Chem. Commun.* **2010**, *46*, 3025−3027. (b) Denton, R. M.; Tang, X.; Przeslak, A. *Org. Lett.* **2012**, *12*, 4678−4681. (c) Denton, R. M.; An, J.; Lindovska, P.; Lewis, W. *Tetrahedron* **2012**, *68*, 2899−2905. (d) Tang, X.; An, J.; Denton, R. M. *Tetrahedron. Lett.* **2014**, *55*, 799−802. (e) Denton, R. M.; An, J.; Adeniran, B.; Blake, A. J.; Lewis, W.; Poulton, A. M. *J. Org. Chem.* **2011**, *76*, 6749−6767.
(24) Nikitin, K. V.; Muller-Bunz, H.; Gilheany, D. G. *Chem. Commun.* **2013**, 1434−1436.
(25) (a) Godfrey, S. M.; McAuliffe, C. A.; Pritchard, R. G.; Sheffield, J. M.; Thompson, G. M. *J. Chem. Soc., Dalton Trans.* **1997**, 4823−4827. (b) Godfrey, S. M.; McAuliffe, C. A.; Mushtaq, I.; Pritchard, R. G.; Sheffield, J. M. *J. Chem. Soc., Dalton Trans.* **1998**, 3815−3818. (c) Godfrey, S. M.; McAuliffe, C. A.; Pritchard, R. G.; Sheffield, J. M. *Chem. Commun.* **1996**, 2521−2522.
(26) We noticed[24] an unusual feature of these compounds in certain X-ray crystal structure determinations: for those with the chloro-bridged phosphonium dications, molecules of solvent and individual halide anions are positioned potentially to effect such nucleophilic attack on the phosphorus.
(27) A related strategy, dependent on diastereotopic isopropyl methyl groups, was used by Baechler and Mislow to measure phophine inversion rates: (a) Baechler, R. D.; Mislow, K. *J. Am. Chem. Soc.* **1970**, *92*, 4758−4759. (b) Baechler, R. D.; Mislow, K. *J. Chem. Soc. Chem. Commun.* **1972**, 185−187.
(28) Oxides **1a**−**3a**, **5a**, and **6a** were synthesized by the reaction of $PhPCl_2$ with *s*-BuMgCl at −78 °C in diethyl ether followed by the addition of the second Grignard reagent at ambient temperature and oxidation of the resulting phosphines in situ with aqueous hydrogen peroxide (see the Supporting Information for details). This approach failed for the more bulky *tert*-butyl-*sec*-butylphenyl oxide **4a** because the phosphine precursor could not be formed directly with the Grignard reagent. Instead, oxide **4a** was synthesized from *tert*-butylethylphenylphosphine oxide **7a** by lithiation with LDA followed by alkylation with ethyl bromide (see the Supporting Information for details).
(29) All phosphine oxides were purified by column chromatography on silica and, in most cases, isolated as 1:1 mixtures of stereoisomers (their separation was insufficient for diastereomeric enrichment). The diastereomeric phosphine oxides were not crystalline, but colorless oils (**1a**−**3a**, **5a**, **6a**) or waxy solids (**4a**) due to the presence of four stereoisomers as evidenced by chiral stationary phase HPLC analysis. The phosphorus NMR spectra of **1a**−**6a** show two closely positioned, within 0.05−1 ppm, signals of diastereomeric oxides (see the Supporting Information for data).
(30) Jesson, J. P.; Meakin, P. *Acc. Chem. Res.* **1973**, *6*, 269−275.
(31) Casarini, D.; Lunazzi, L.; Mazzanti, A. *Eur. J. Org. Chem.* **2010**, *11*, 2035−2056.
(32) (a) Minegishi, S.; Loos, R.; Kobayashi, S.; Mayr, H. *J. Am. Chem. Soc.* **2005**, *127*, 2641−2649. (b) Lancaster, N. L.; Welton, T.; Young, G. B. *J. Chem. Soc., Perkin Trans. 2* **2001**, *12*, 2267−2270.
(33) de la Mare, P. B. D. *J. Chem. Soc.* **1955**, 3180−3187.
(34) Perrin, C. L.; Dwyer, T. J. *Chem. Rev.* **1990**, *90*, 935−967.
(35) Marenich, A. V.; Olson, R. M.; Kelly, C. P.; Cramer, C. J.; Truhlar, D. G. *J. Chem. Theory Comput.* **2007**, *3*, 2011−2033.
(36) (a) More O'Ferrall, R. A. *J. Chem. Soc. B* **1970**, 274−277. (b) Jencks, W. P. *Chem. Rev.* **1972**, *72*, 705−718. (c) Sato, M.; Yamataka, H.; Komeiji, Y.; Mochizuki, Y. *Chem.—Eur. J.* **2012**, *18*, 9714−9722.
(37) (a) Kamerlin, S. C. L.; McKenna, C. E.; Goodman, M. F.; Warshel, A. *Biochemistry.* **2009**, *48*, 5963−5971. (b) Edwards, D. R.; Brown, R. S. *Biochim. Biophys. Acta* **2013**, *1834*, 433−442.